

AD-A210 658

4

Final Report

Contract N00014-88-K-0275

Work Unit No. 4311922

EXPLORATORY STUDY OF NIOBIUM, TITANIUM, ZIRCONIUM AND TANTALUM ALUMINIDES

for the period 88/3/1/ - 89/5/31

N.S. Stoloff  
Materials Engineering Department  
Rensselaer Polytechnic Institute  
Troy, NY 12180-3590

DTIC  
ELECTE  
AUGO 1 1989  
S B D

July 1, 1989

DISTRIBUTION STATEMENT A

Approved for public release;  
Distribution Unlimited

## ABSTRACT

The microstructure, crystal structures of existing phases, hardness and slip systems for several binary and ternary aluminides have been determined. Arc melted samples purchased from an external supplier invariably cracked upon cooling in the arc melting unit, thereby hampering the ability to prepare mechanical test specimens. Homogenization heat treatments in vacuum usually led to significant porosity, apparently due to loss of aluminum. The properties of arc melted material are compared to those derived from similar compositions prepared by powder metallurgical techniques. J20 ←

### I. INTRODUCTION

The mechanical properties and operative slip/or twinning modes of aluminides based on titanium and nickel and iron have been well characterized. Although considerable success has been achieved in improving strength, oxidation resistance and ductility of these aluminides, none appear capable of competing with current nickel base superalloys for high temperature structural applications. Rather, the titanium aluminides TiAl and Ti<sub>3</sub>Al exhibit low density coupled with reasonable strength to 760°C. Single phase Ni<sub>3</sub>Al, suitably alloyed with boron and various solid solution additions, is comparable in strength to early  $\gamma/\gamma'$  superalloys which contain low volume fractions of the strengthening  $\gamma'$  phase.

Since the need for superalloy replacements cannot be met by the aluminides described above, new compounds have been sought which, though brittle, might provide sufficient plasticity to serve as the matrix for composites. The need for oxidation resistance is paramount. Also, low density is an important consideration. Therefore, the

on For  
A&I ☒  
ed ☐  
tion ☐

tion/  
Availability Codes

Dist	Avail and/or Special
A-1	

aluminides  $\text{Al}_3\text{Ta}$  and  $\text{Al}_3\text{Nb}$  were chosen for initial study in this program. A recently revised phase diagram for Al-Ta is shown in Fig. 1[11]. Later, alloys based upon  $\text{Al}_3\text{Ti}$  and  $\text{Al}_3\text{Zr}$  also were screened. All of these alloys display tetragonal  $\text{D}_{022}$  superlattice structures except for  $\text{Al}_3\text{Zr}$ , which is  $\text{D}_{023}$ .

## II. ALLOYS AND EXPERIMENTAL PROCEDURES

Alloys listed in Table 1, prepared by arc melting, were purchased from General Electric Co. Corporate Research and Development Center:

Of these, only two, binary  $\text{Al}_3\text{Ti}$  and  $\text{Al}_3\text{Zr}$ , were received without cracks. In addition, all contained casting pores. Metallographic, microprobe and x-ray analyses indicated that none of the samples was homogeneous. The poor condition of most of the arc melted ingots, together with their extreme brittleness, precluded machining of compression or bend samples from any of the ingots. However, some samples of  $\text{Al}_3\text{Ta}$  prepared by powder metallurgical techniques (hot isostatic pressing) were machined into compression samples.

## III. EXPERIMENTAL RESULTS

### A. Microstructures

The nominally  $\text{Al}_3\text{Ta}$  sample, Fig. 2, contained a second phase corresponding to  $\text{Al}_2\text{Ta}$ . The composition of the major  $\text{Al}_3\text{Ta}$  phase was determined by microprobe to be  $23.6 \pm 0.2\% \text{Ta}$ , in close agreement with a recently reported value[1] for this line compound.

Samples of  $\text{Al}_3\text{Ta}$  with 8a%Fe, 8%Ni or 10%Ni were analyzed by microprobe, with the results shown in Table 2. The addition of iron produced a three phase mixture: a solid solution of 0.5a%Fe in  $\text{Al}_3\text{Ta}$ , a ternary phase which could not be identified, and  $\text{Al}_3\text{Fe}$ , see Figs. 3a) and b).

Samples of  $\text{Al}_3\text{Ta}$  with 8 or 10% nickel also contained three phases. The compositions of phases were similar for both alloys, consisting of a ternary phase, a solid solution of  $\text{Al}_3\text{Ta}$  with 1a%Ni and  $\text{Ni}_2\text{Al}_3$ , Fig. 4. The sample with 10%Ni simply contained more  $\text{Ni}_2\text{Al}_3$ . As with the iron-containing alloy, the x-ray diffraction pattern could not be identified, but is assumed to be orthohombic, as predicted by Pettifor's<sup>[2]</sup> structure map for  $\text{A}_2\text{B}$  alloys.

Representative microstructures obtained for several other alloys listed in Table 1 are shown in Fig. 5a)-g). In every case at least two phases were observed, even for binary  $\text{Al}_3\text{Zr}$ , Fig. 5a). Note that the addition of 8Ni to  $\text{Al}_3\text{Zr}$ , Fig. 5b), caused the formation of at least three phases.

#### Heat Treatments

Various heat treatments were attempted to homogenize the samples and induce grain growth.  $\text{Al}_3\text{Ta}$ , heated for 48 hours in argon at  $1500^\circ\text{C}$ , reacted with the alumina crucible, oxidized, and exhibited increased porosity. In addition, the amount of Ta-rich phase increased.

Annealing of  $\text{Al}_3\text{Ta}$  at  $1200^\circ\text{C}$  for four hours did not homogenize the alloy, caused preferential interdendritic oxidation and coarsening of internal porosity, see Fig. 6. HIPing for 4 hours at  $1200^\circ\text{C}$  under a pressure of 69MPa helped eliminate some of the porosity, although the samples still oxidized and were not homogeneous.

Heat treating the ternary  $\text{Al}_3\text{Ta}$  samples at  $1100^\circ\text{C}$  for 24 hours in vacuum eliminated the nickel and iron-enriched phases, but the samples still displayed oxidation and internal porosity.

Heat treatment of the other binary and ternary intermetallics listed in Table 1 also resulted in increased porosity. Microprobe measurements of alloy compositions suggested that at least a portion of this porosity was due to loss of aluminum during heat treatment.

#### Hardness

Hardness values were obtained for all alloys listed in Table 1. The hardnesses of binary  $\text{Al}_3\text{Ti}$ ,  $\text{Al}_3\text{Zr}$  and  $\text{Al}_3\text{Ta}$  were similar, in the range 370-407 DPH.  $\text{Al}_3\text{Nb}$  displayed an average of about 500 DPH. In the case of  $\text{Al}_3\text{Ta}$  with Fe or Ni additions, Table 2, hardnesses were obtained for at least one phase in addition to the  $\text{Al}_3\text{Ta}$  phase. Table 2 shows that the unidentified Fe and Ni-rich ternary phases had much higher hardnesses than did  $\text{Al}_3\text{Ta}$ . The maximum hardness noted was 766DPH for the ternary phase in the alloy containing 8%Ni. Heat treatment led to changes in hardness of the coexisting phases, as shown in Table 3, but no consistent trends were noted.

#### Slip Bands at Hardness Impressions

In general, slip bands could not be resolved around hardness impressions, but in the case of  $\text{Al}_3\text{Nb}$  a few faint bands were seen, see Fig. 7. However, we were unable to identify the slip planes. Hardness impressions in other alloys also have been examined for the presence of slip bands. Fig. 8a) shows slip bands around impressions in Al-25Ta-8Fe. Again these could not be identified.

Cracks usually were noted around hardness impressions in the matrix of Al-25Ta-10Fe, see Fig. 8b). A distributed island phase, lower left of Fig. 8b), was softer: DPH 713 vs 352 for the matrix, and exhibited no cracking. The soft island phase had composition

75.8%Al, 0.15%Fe, 23.9%Ta, corresponding to  $\text{Al}_3\text{Ta}$ . In spite of the lack of cracking, no slip traces were observed.

#### Compression Tests

Since the arc melted buttons did not provide material suitable for compression testing, several powder compacts of Al-Ta and Al-X-Ta compositions were prepared by powder techniques: hot isostatic pressing (HIPing) of elemental powder at 1200°C. Compression samples were machined as right circular cylinders 1/8" dia x 1/4" high or 3/16" dia x 3/8" high. End surfaces were lapped so that they were parallel to each other and at right angles to the side. Samples were lightly ground with 600 grit SiC paper. Tests were carried out at in the range 25-950°C, see Table 3. A yield stress could only be measured at 850°C and 950°C, while stresses to fracture were recorded at 25 and 750°C. Fracture surfaces are shown in Figs. 9 and 10 for 25°C and 750°C, respectively.

#### IV. DISCUSSION

Additions of Ti, Fe, Cu and Ni are predicted by Pettifor[2], to produce  $\text{L}_{12}$  crystal structures in  $\text{DO}_{22}$  and  $\text{DO}_{23}$  compounds such as those chosen for the present study, see Fig. 11. Others have indeed succeeded in transforming  $\text{DO}_{23} \text{Al}_3\text{Zr}$ [3] and  $\text{DO}_{22} \text{Al}_3\text{Ti}$ [4,5] to the  $\text{L}_{12}$  structure, but no improvement in ductility was observed. Efforts to stabilize the  $\text{L}_{12}$  structure in  $\text{Ti}_3\text{Al}$ [6] and  $\text{Al}_3\text{Nb}$ [3] have reportedly been unsuccessful. The present work confirms that ductility improvements cannot be achieved through the addition of transition elements, whether or not the crystal structure is modified.

There are several possible explanations of why Pettifor's structure

maps predicted incorrectly the crystal structure of  $\text{Al}_3\text{Ta}$  with ternary additions of nickel and iron. First, Pettifor's maps do not account for regions in which two phases are stable. The additions most likely substituted for both Ta and Al rather than only Al, making the ternary phase a transformation of the  $\text{Al}_2\text{Ta}$  phase. Although the planes could not be indexed to fit a Bravais lattice system, it is hypothesized that the ternary phase is a complex orthorhombic structure which would explain both the increase in hardness and the complex diffraction pattern. Extensive TEM work would be necessary to confirm this hypothesis. The increase in hardness of the solid solution phases and the decrease in lattice parameters resulted directly from the lattice strains caused by the size misfit of the iron and nickel atoms in the  $\text{Al}_3\text{Ta}$  matrix. The size misfit of nickel is larger than that of iron which explains why nickel strengthens more than iron.

Other researchers have observed an increase in porosity after heat treating cast or P/M intermetallics and have suggested possible explanations including:

- o the loss of aluminum due to its high vapor pressure,
  - o void formation as a result of the homogenization of second phases, and
  - o the formation of pores due to entrapped oxygen and hydrogen.
- Anton<sup>[7]</sup> calculated that even HIPing at 207MPa could leave 1v% pores containing entrapped gasses. Clearly, all these explanations may apply to  $\text{Al}_3\text{Ta}$ . Several powder samples experienced a loss in weight during sinterings, supporting the first hypothesis.

## V. SUMMARY AND CONCLUSIONS

Arc melting of DO<sub>22</sub> aluminides based upon Al<sub>3</sub>Ta and Al<sub>3</sub>Nb leads to severe cracking on cooling. Better results are obtained through powder techniques. Buttons of Al<sub>3</sub>Ti and Al<sub>3</sub>Zr can be prepared by arc melting without cracking. All alloys were brittle at room temperature, as established by cracking around hardness impressions or by compression tests. Al<sub>3</sub>Ta alloys showed some plasticity in compression at 750, 850 and 950°C.

Arc melted samples of binary and ternary Al<sub>3</sub>Ta alloys exhibited two or more phases usually with widely differing hardnesses. Homogenization heat treatments cause increased porosity. Slip markings were seen around room temperature hardness impressions in single phase Al<sub>3</sub>Nb and in multiphase Al<sub>3</sub>Ta and its alloys, but the slip planes could not be identified.

Producing L1<sub>2</sub> compounds by means of ternary alloying additions does not produce appreciable ductility in any of the alloys studied.



#### IV. REFERENCES

1. P.R. Subramanian, D.B. Miracle and S. Mazdiasni, submitted to Metall. Trans. A, 1988.
2. D.G. Pettifor, J. of Physics, V. 19, p. 289, 1986.
3. J. Schneibel and W. Porter, in High Temperature Ordered Intermetallic Alloys II, MRS Pittsburgh, PA, 1989, in press.
4. E.P. George, W.D. Porter, H.M. Henson, W.C. Oliver and B.F. Oliver, in High Temperature Ordered Intermetallic Alloys, III, MRS, Pittsburgh, PA, 1989, in press.
5. W.D. Porter, K. Hisatsune, C.J. Sparks and W.C. Oliver, in High Temperature Ordered Intermetallic Alloys III, MRS, Pittsburgh, PA, in press, 1989.
6. C.T. Liu, J. Horton and D.G. Pettifor in High Temperature Ordered Intermetallic Alloys III, MRS, Pittsburgh, PA, 1989 in press.
7. D. Anton in High Temperature/High Performance Composites, MRS Symposia V. 120, Pittsburgh, PA, 1988, p. 57.

**Table 1**  
List of Alloys

Alloy No	Nominal Composition	General Condition	VHN (50gf)
1	Al <sub>3</sub> Ti	OK	378
2	Al <sub>3</sub> Zr	OK (brittle)	407
3	(Al-8Ni)-25Zr	cracked	376-623
4	(Al-8Fe)-25Ta	cracked	473-655
5	(Al-8Fe)-25Ti	cracked	265
6	(Al-8Cu)-25Ta	cracked	454
7	(Al-8Ti)-25Ta	cracked	412-720
8	(Al-8Fe)-25Nb	cracked	509-638
9	(Al-10Fe)-25Ta	cracked	435-713
10	(Al-8Ni)-25Ti	cracked	299
11	Al <sub>3</sub> Ta	cracked	370
12	Al <sub>3</sub> Nb	cracked	500

Table 2

Composition and Hardness of Phases in Al-25%Ta

	<u>Composition (a%)</u>				<u>DPH</u>
	Ta	Al	Ni	Fe	
Al <sub>3</sub> Ta with Fe(8%)					
ternary phase	32	56	-	12	571
Al <sub>3</sub> Ta phase	23	76	-	0.5	391
Al <sub>3</sub> Fe phase	1	78	-	21	-
Al <sub>3</sub> Ta with Ni(8%)					
ternary phase	30	58	12	-	766
Al <sub>3</sub> Ta phase	22	77	1	-	437
Ni <sub>2</sub> Al <sub>3</sub> phase	0	62	38	-	-
Al <sub>3</sub> Ta with Ni(10%)					
ternary phase	31	57	12	-	672
Al <sub>3</sub> Ta phase	22	77	1	-	441
Ni <sub>2</sub> Al <sub>3</sub> phase	0	62	38	-	-
Al <sub>3</sub> Ta	23.6	76.4	-	-	370

**Table 3**

Compression Tests on Al-Ta Alloys

Composition	T °C	$\sigma_{ys}$ (MPa)	$\sigma_F$ (MPa)
Al-23Ta	25		286
Al-24Ta	25		497
Al-25Ta	25		531
Al-25Ta-8Fe	25		372
Al-24Ta	750		439
Al-25Ta-8Fe	750	748	
Al-25Ta-8Fe	850	701	
Al-23Ta	950	239	
Al-25Ta	950	41	
Al-25Ta-8Fe	950	198	

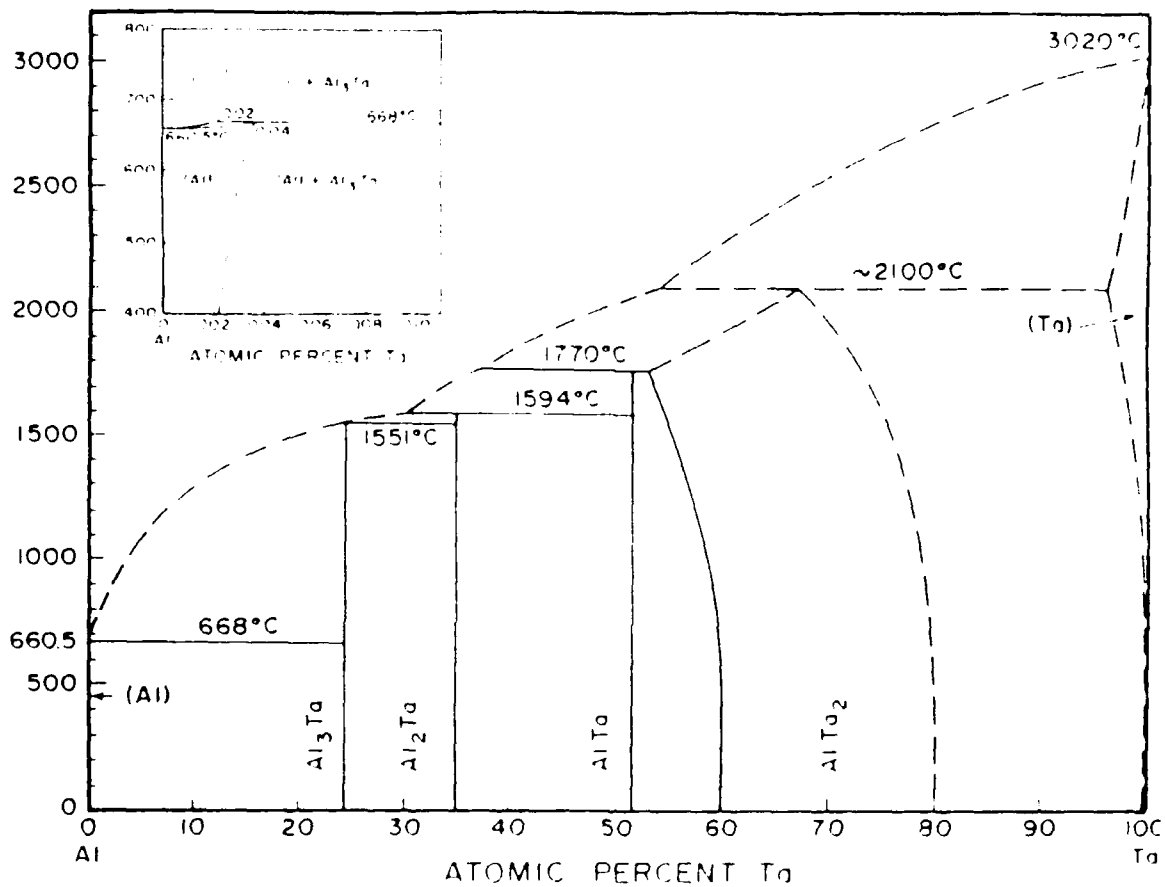
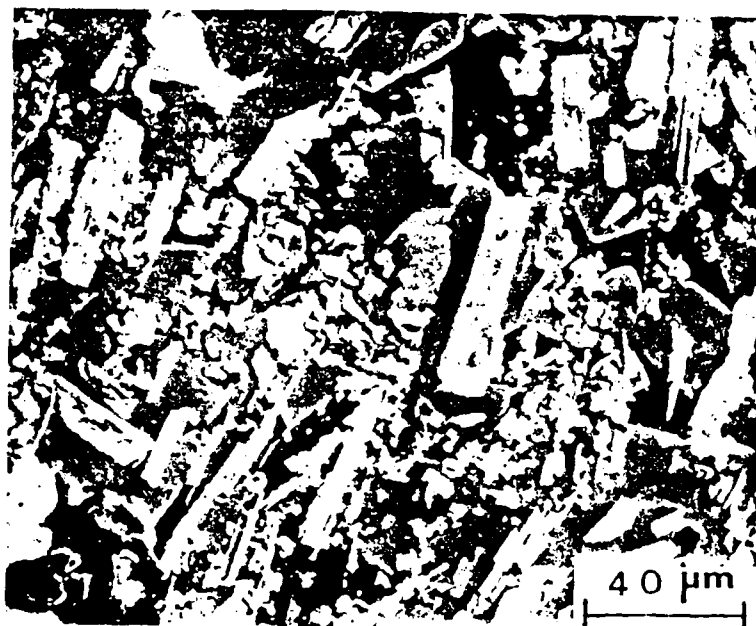
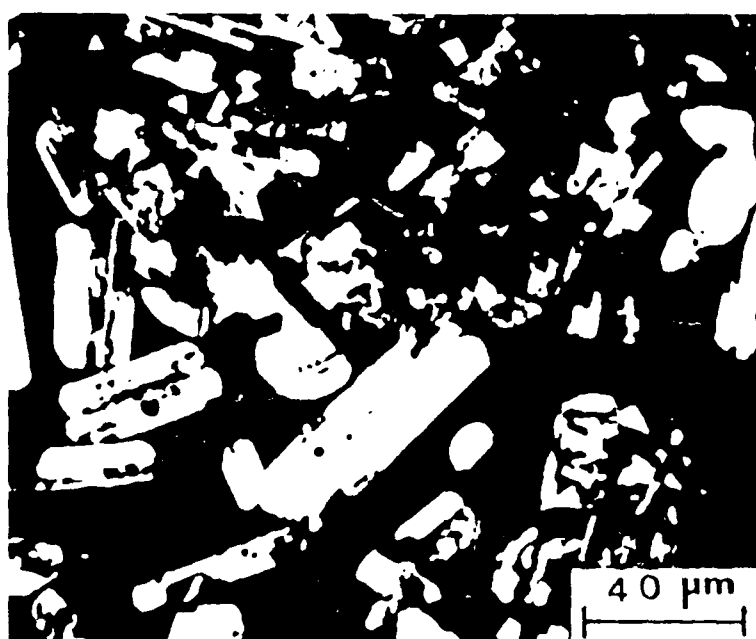


Fig. 1 Revised Al-Ta phase diagram[1].



a)



b)

Fig. 2 Arc melted Al-25Ta, annealed 48 h at 1500°C. a)  $\text{Al}_3\text{Ta} + \text{Al}_2\text{Ta}$  (probe sample) b) back scattered electrons.

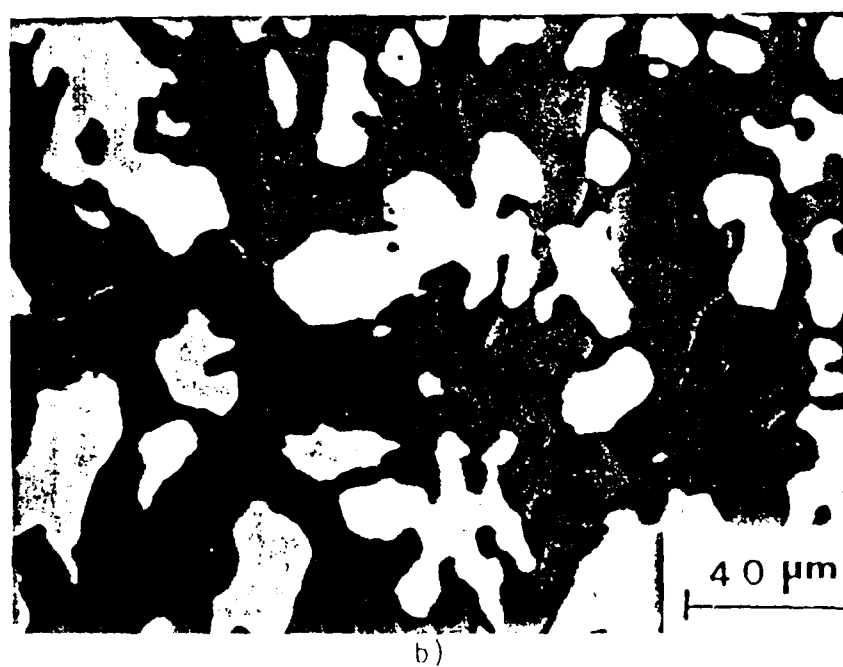
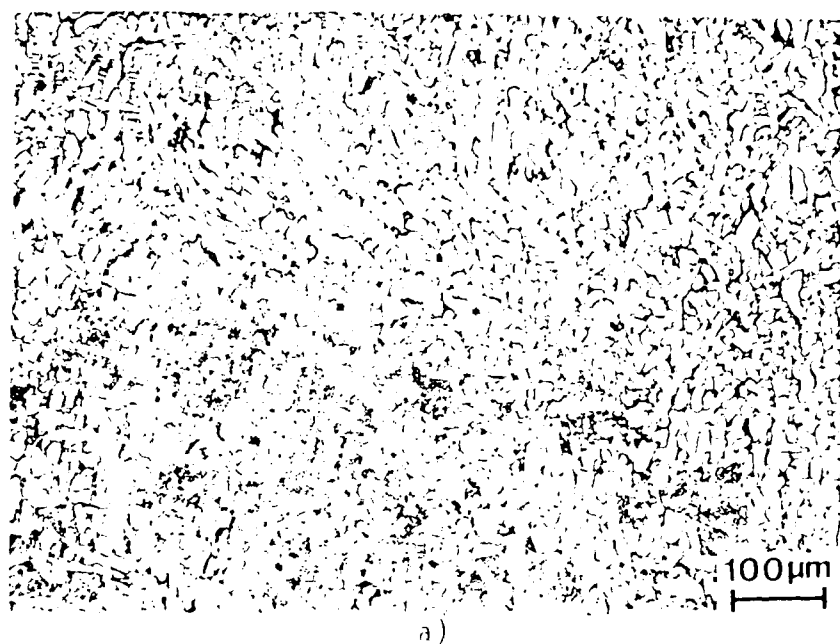


Fig. 3 Microstructure of arc melted Al-8Fe-25In  
 a) an etched, optical b) back scattered  
 SEM. Black phase is  $Al_3Fe$ , dark gray phase  
 is  $Al_3In$ , light gray phase is ternary.

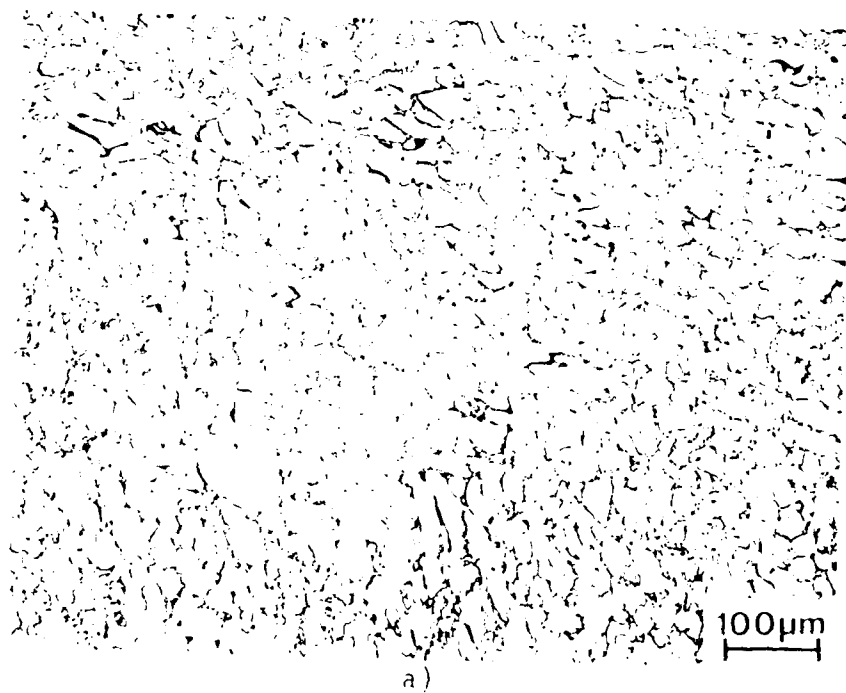


Fig. 4 Microstructures of arc melted Al-5Ni-25Ta  
 a) etched, optical b) back scattered SEM.  
 The black phase is  $\text{Ni}_2\text{Al}_3$ , dark gray phase  
 is  $\text{Al}_3\text{Ta}$ , light gray phase is ternary.



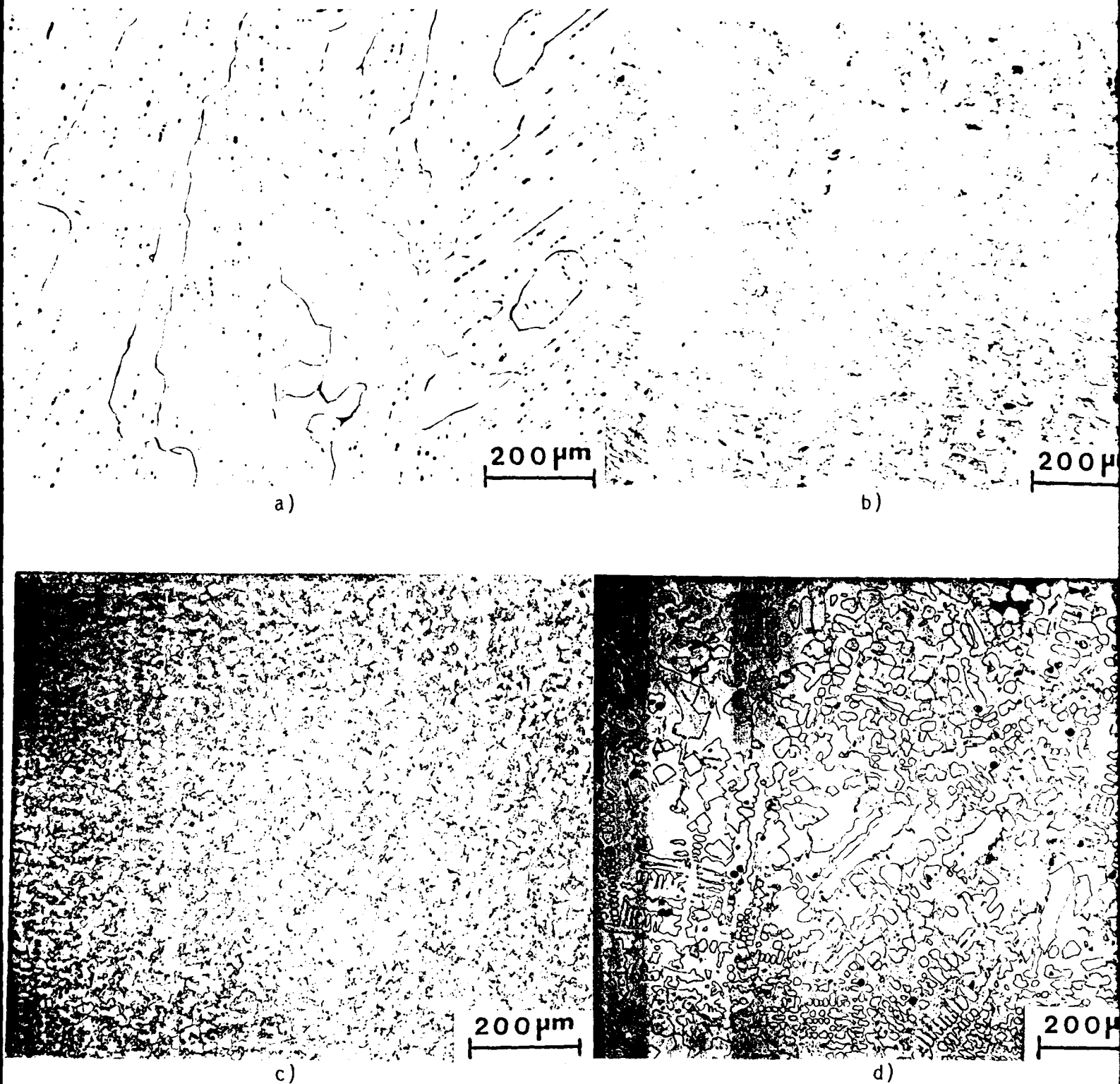
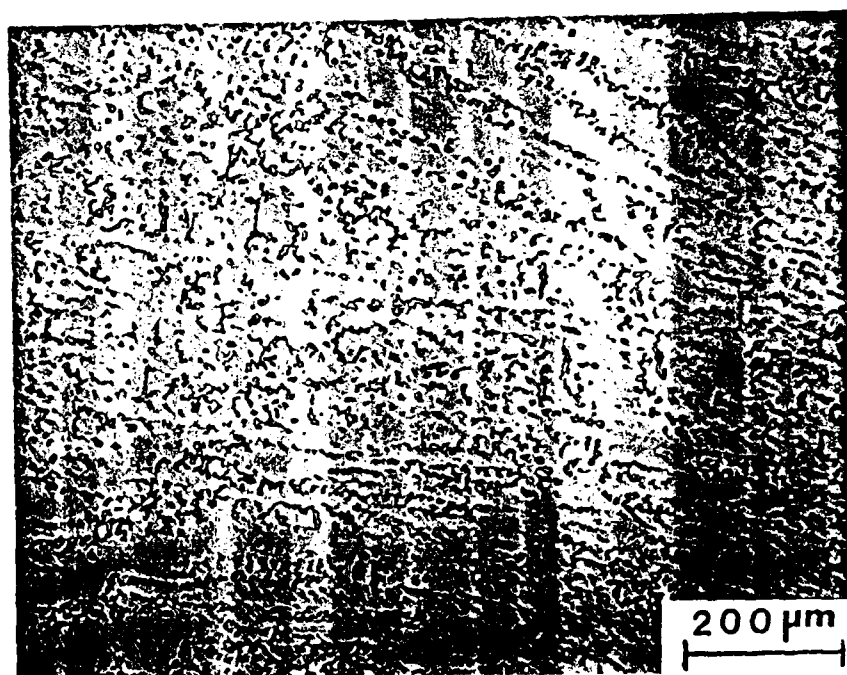


Fig. 5 Microstructures of arc melted ingots  
 a) Al-25Zr, b) Al-8Ni-25Zr, c) Al-8Cu-25Ta  
 d) Al-8Ti-25Ta, e) Al-8Fe-25Ta f) Al-8Fe-25Ti  
 g) Al-8Ni-25Ti



g)

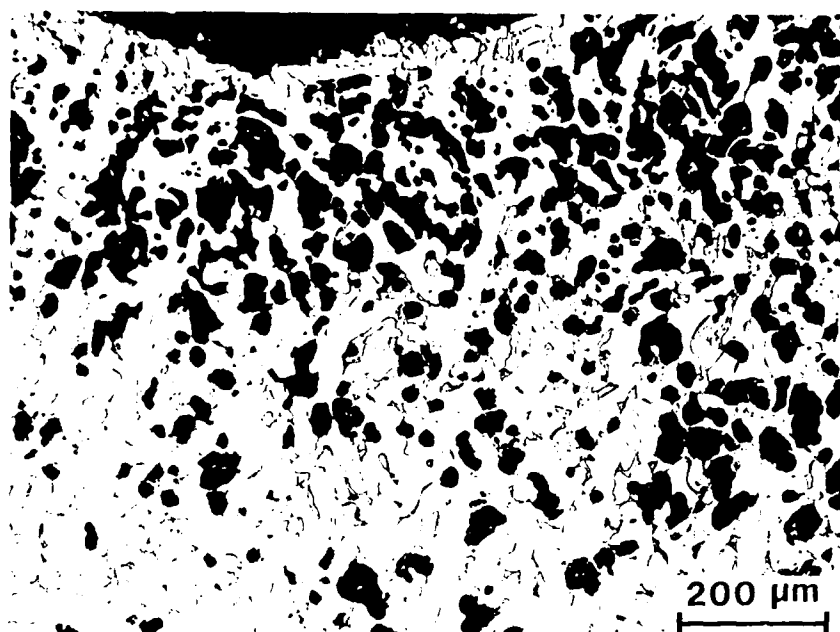
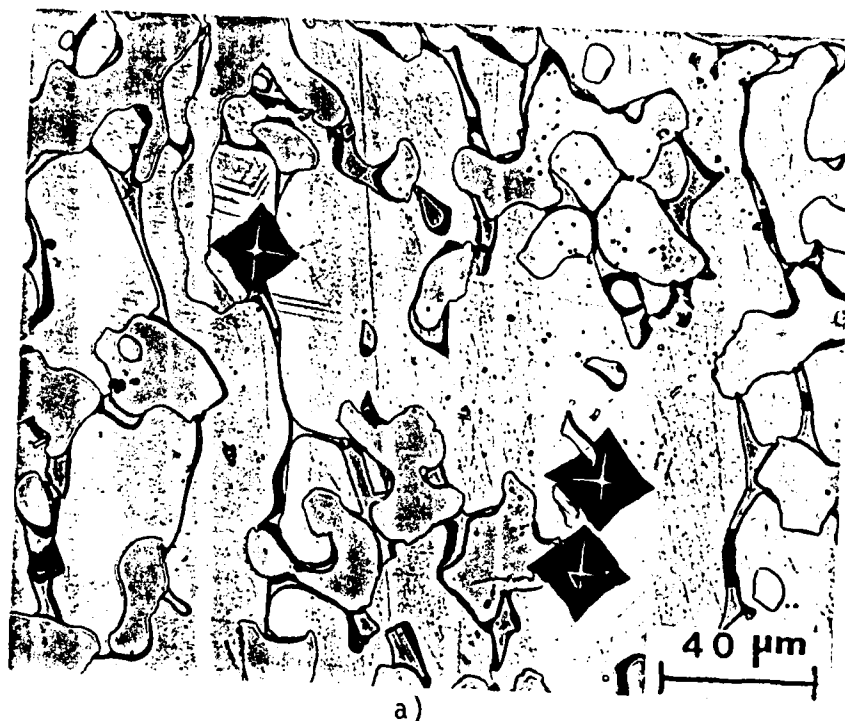


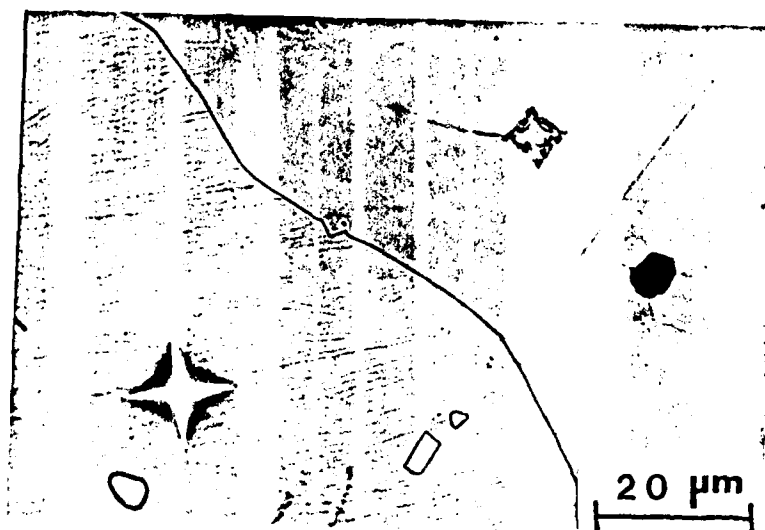
Fig. 6 Outer surface of arc cast  $\text{Al}_3\text{Ta}$  annealed 4 h at  $1200^\circ\text{C}$  in argon.



Fig. 7 Slip bands around hardness impressions in arc melted  $\text{Al}_3\text{Nb}$ .

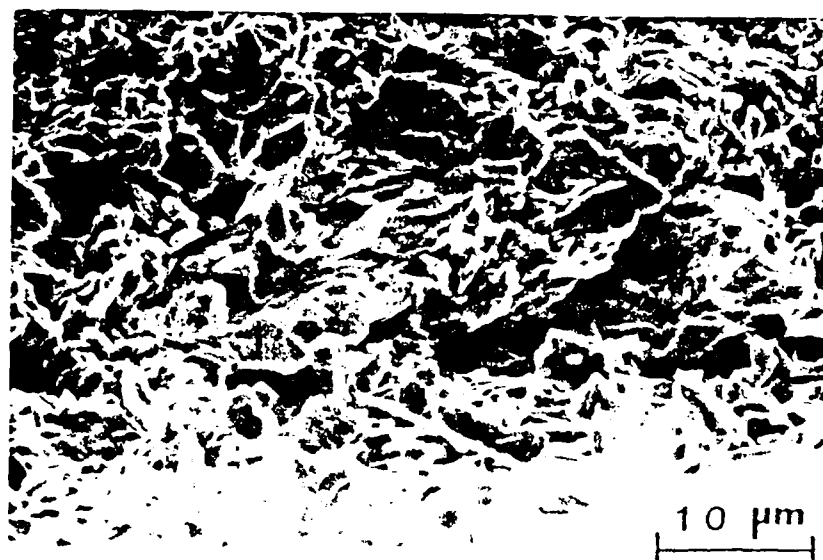


a)

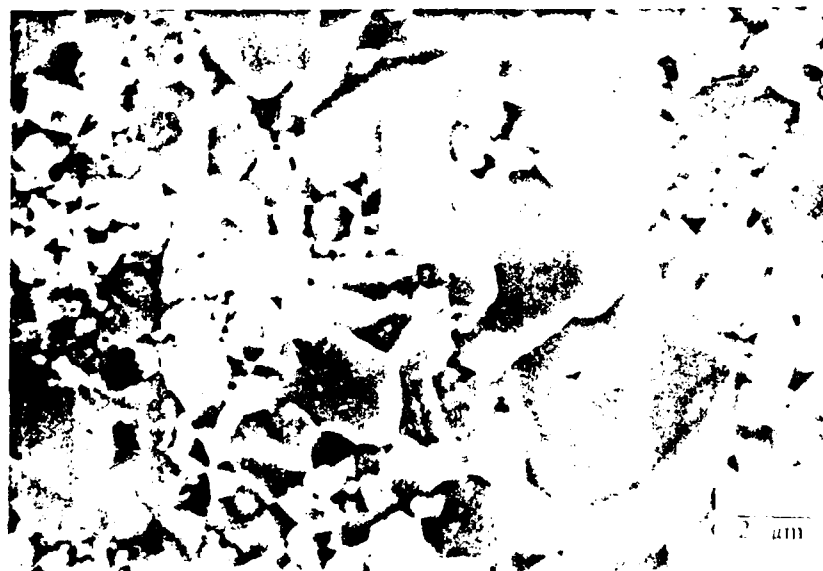


b)

Fig. 8 Hardness impressions in arc melted  $\text{Al}_3\text{Ta}$  alloys a) Al-8Fe-25Ta  
b) Al-10Fe-25Ta



a)



b)

Fig. 9 Fracture surface of P/M Al-Ta alloys, tested in compression at 25°C a) Al-25Ta  
b) Al-8Fe-25Ta

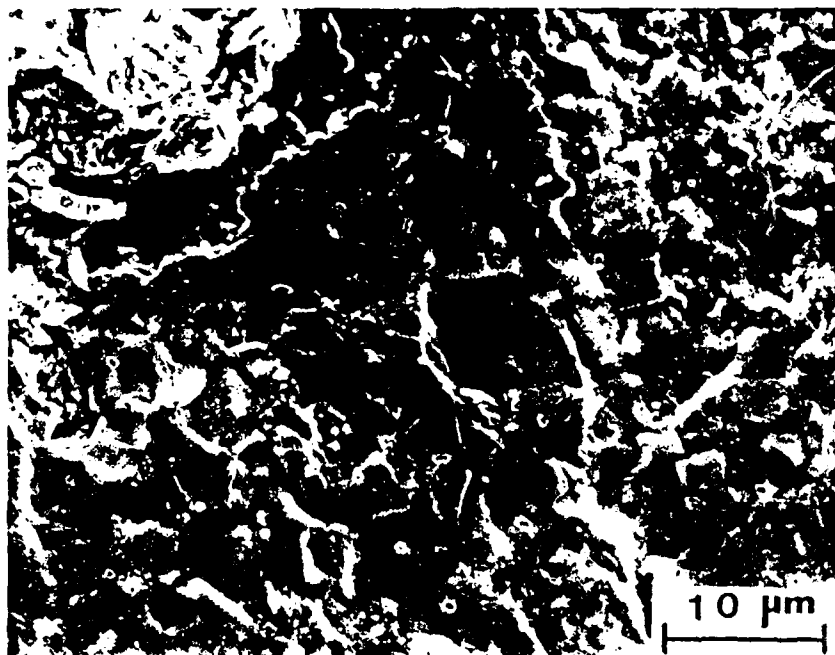


Fig. 10 Fracture surface of P/M Al-24Ta  
tested in compression at 750°C.

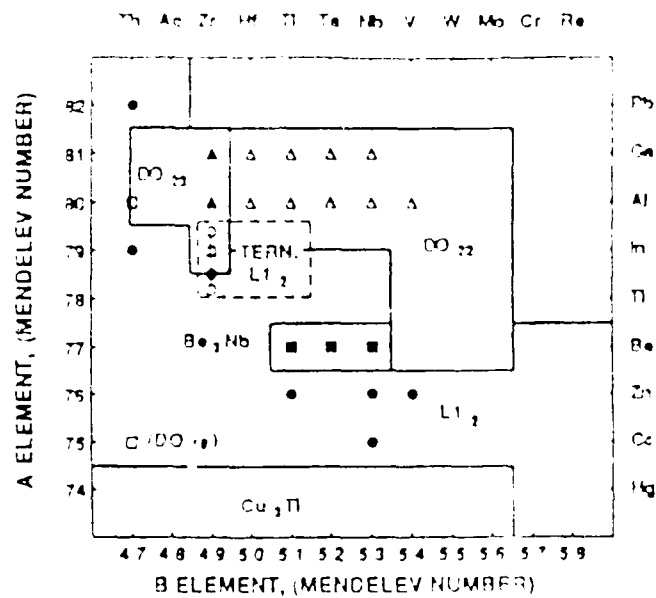


Fig. 11 Pettifor[2] structure map for B02 phase field.

UNCLASSIFIED

SECURITY CLASSIFICATION OF THIS PAGE

REPORT DOCUMENTATION PAGE

Form Approved  
OMB No. 0704-0188

REPORT SECURITY CLASSIFICATION UNCLASSIFIED			1b RESTRICTIVE MARKINGS		
SECURITY CLASSIFICATION AUTHORITY			3 DISTRIBUTION/AVAILABILITY OF REPORT Distribution unlimited		
DECLASSIFICATION/DOWNGRADING SCHEDULE					
PERFORMING ORGANIZATION REPORT NUMBER(S)  N00014-88-K-0275-1			5 MONITORING ORGANIZATION REPORT NUMBER(S)		
1. NAME OF PERFORMING ORGANIZATION Rensselaer Polytechnic Institute		6b OFFICE SYMBOL (If applicable)		7a NAME OF MONITORING ORGANIZATION Office of Naval Research	
2. ADDRESS (City, State, and ZIP Code)  Troy, NY 12180-3590				7b ADDRESS (City, State, and ZIP Code) Materials Division, Code 1131M, 800 N. Quincy St., Arlington, VA 22217-5000	
3a. NAME OF FUNDING/SPONSORING ORGANIZATION		3b OFFICE SYMBOL (If applicable) N62927		9 PROCUREMENT INSTRUMENT IDENTIFICATION NUMBER  N00014-88-K-0275	
3c. ADDRESS (City, State, and ZIP Code)		10 SOURCE OF FUNDING NUMBERS			
		PROGRAM ELEMENT NO		PROJECT NO	TASK NO
					WORK UNIT ACCESSION NO
11. TITLE (Include Security Classification)  EXPLORATORY STUDY OF NIOBIUM, TITANIUM, ZIRCONIUM AND TANTALUM ALUMINIDES (Unclassified)					
12. PERSONAL AUTHOR(S) Stoloff, Norman S.					
13a. TYPE OF REPORT Final		13b. TIME COVERED FROM 88/3/1 TO 89/5/31		14 DATE OF REPORT Year, Month, Day 89/7/1	
				15 PAGE COUNT 23	
16. SUPPLEMENTARY NOTATION					
17. COSATI CODES			18 SUBJECT TERMS (Continue on reverse if necessary and identify by block number)		
FIELD	GROUP	SUB-GROUP	aluminides, arc melting microprobe analysis		
			fracture phases		
			intermetallic compounds slip		
19. ABSTRACT (Continue on reverse if necessary and identify by block number) The microstructure, crystal structures of existing phases, hardness and slip systems for several binary and ternary aluminides have been determined. Arc melted samples purchased from an external supplier invariably cracked upon cooling in the arc melting unit, thereby hampering the ability to prepare mechanical test specimens. Homogenization heat treatments in vacuum usually led to significant porosity, apparently due to loss of aluminum. The properties of arc melted material are compared to those derived from similar compositions prepared by powder metallurgical techniques.					
20 DISTRIBUTION/AVAILABILITY OF ABSTRACT <input checked="" type="checkbox"/> UNCLASSIFIED/UNLIMITED <input type="checkbox"/> SAME AS RPT <input type="checkbox"/> DTIC USERS			21 ABSTRACT SECURITY CLASSIFICATION UNCLASSIFIED		
22a. NAME OF RESPONSIBLE INDIVIDUAL			22b TELEPHONE (Include Area Code)		22c OFFICE SYMBOL